Mapping of the indoor comfort conditions considering the effect of solar radiation

Concettina Marino[1,*], Antonino Nucara[1] , Matilde Pietrafesa[1]

[1] DIIES – Dipartimento di Ingegneria di Ingegneria dell'Informazione, delle Infrastrutture e dell'Energia Sostenibile - University "Mediterranea" of Reggio Calabria, Reggio Calabria, Italy

[*]Corresponding email: concettina.marino@unirc.it

Keywords: solar radiation, mean radiant temperature, thermal comfort, building energy consumption

ABSTRACT

This paper investigates the influence of solar radiation on thermal comfort inside an indoor environment and its effect on the building energy consumptions. Furthermore, it draws up a procedure which allows the rating of the thermal comfort quality of indoor environments in the presence of solar radiation, to be used in correlation with the energy classification of building in order to refer the energy performance to the indoor environmental conditions.

Mean Radiant Temperatures (MRT) for a subject exposed to solar radiation in different positions of the environment were calculated, with an hourly time step and for a whole year. These values were utilized to assess the Predicted Percentage of *Dissatisfied* (PPD) and its variation with time and space, so that long term thermal comfort evaluations were able to be carried out and comparisons among irradiated and not irradiated positions were able to be made.

1 INTRODUCTION

Nowadays the current need to restrain both energy consumptions and the consequent pollutant emission releases into the environment has often led governments to undertake policies focused on limiting energy demand of buildings. In the effort of designing efficient buildings, the primary objective of edifices, which is providing shelter and comfort for people that live work and interact in them, should not be neglected. This is mainly for two reasons: 1) in office buildings comfort of occupants has a significant influence on the productivity, abstention and could cost in terms of working hours [1, 2]; 2) occupants react to any perceived discomfort by taking actions to restore their comfort but sometimes these actions may enhance energy cost. Therefore, it is important to recognize that a 'low energy' standard that increases occupant discomfort may be no more sustainable than one that encourages energy use [3].

This issue has been entirely received by the 2002/91/EC Directive of the European Parliament and of the Council on the energy performance of buildings [4] and by the 2010/31/EU European Directive [5], which, drawing up a methodology leading to buildings energy certification, strongly highlights the link between energy saving purposes and comfort of occupants of indoor environments.

From this point of view thermal comfort should be considered the most relevant facet of the issue because it directly affects both building energy performance and productivity in indoor environments [6-8].

Several approaches have been developed for the last few years to assess thermal comfort. Usually they take into account the primary environmental and personal factors that affects thermal interaction between the body and surrounding environment [9-12], whereas the behaviour of occupants has been introduced by the adaptive approach [3, 13, 14].

Currently the model proposed by Fanger [9], based on PMV and PPD indexes, is widely used for practical application and is largely accepted for design and field assessment of comfort conditions. As a matter of fact the model has been adopted by the EN 15251 technical standard [15] delineating "how to establish and define the main parameters to be used as input for building energy calculation and long term evaluation of the indoor environment". In particular, as far as thermal facet is concerned, EN 15521 refers to ISO 7730 Standard [16] linking the classification of thermal environments to the values of PMV and PPD indexes.

As regards the radiant field, it is largely acknowledged the thermal sensation experienced by a subject in a confined environment is significantly affected by the radiative heat exchange.

The parameter that rules the radiant heat exchange between human body and surrounding environment is the mean radiant temperature (MRT) whose influence on thermal comfort is well documented [17-20].

The effect of MRT on the energy consumption has been also investigated by Kang et al. [21] who analyzed the energy saving potential in a PMV-controlled space. The results suggested that, although energy-saving potential is reduced under the high mean radiant temperature condition, the thermal comfort control is still a reasonable strategy to achieve both thermal comfort and energy saving simultaneously.

Therefore the accurate assessment of radiant field and MRT is crucial for both comfort and energy savings purposes. Nevertheless, despite this evidence, there is also a lack of studies addressing the influence of a type of radiant sources which strongly affect the radiant field and alter the MRT: they are known as high intensity radiation sources and the sun is the most important example.

Indeed experimental analysis have demonstrated that solar radiation is a significant cause of discomfort to people [22], but there are few models [23] allowing analytical assessment of MRT taking into account solar radiation.

In this work we use a comprehensive method for the computation of mean radiant temperature values in thermal moderate indoor environments in the presence of solar radiation.

These values have been utilized to assess the Predicted Mean Vote (PMV) and its variation with time and space into a selected environment, so that long term thermal comfort evaluations have been carried out and comparisons among irradiated and not irradiated positions have been made.

The obtained results have been exploited to realize the classification of the thermal comfort quality of the environment by means of a procedure [25], which takes into account long term evaluations.

Therefore the work designs a procedure which, allowing the rating of the thermal comfort quality of indoor environments during a selected period of time, can be used in correlation with energy classification of building in order to refer energy performances to indoor environmental conditions, bringing into effect one of the pivotal statement of the 2010/31/EU European Directive [5].

2 METHODOLOGY

The innovative aspect of that procedure proposed in this research regards the consideration of solar radiation and its effect on comfort of irradiated subjects.

As a matter of fact we used a comprehensive method for the computation of the mean radiant temperature (MRT) which takes into account solar radiation crossing glazed surfaces and entering the moderate thermal environments [24]. These MRT values are utilized to assess the Predicted Percentage of *Dissatisfied* (PPD), along with its variation with time and space, so that long term thermal comfort evaluations may be carried out and comparisons among irradiated and not irradiated subject's positions may be effected.

The obtained results allow to realize the classification of the thermal comfort quality of the environment by means of a quality index, named Environmental Quality Index [25], that was singled out and used to assess the comfort quality of indoor environments over long periods of time (namely one year).

Consequently a transient regime analysis is needed to assess environmental parameters describing indoor environmental conditions (air temperature, temperatures of internal wall surfaces) and their variation with time.

This analysis permits to properly take into account the effect of both the climate variability and building envelope characteristics on the indoor environmental conditions and, generally, can be performed by means of field measurement campaigns or simulation tools.

A simulation tool was used in the present study; it is one of the most versatile software for research purpose: EnergyPlus [26].

Its structure consists of many program modules working together and controlled by the Integrated Solution Manager. As a consequence all the parts of the building-plant system can be simulated simultaneously and the energy demand is calculated at the end of an iterative process where every module gives feedback to the others. This configuration, where the elements are linked in a simultaneous solution scheme, allows physically realistic simulations provided that input data and the whole process is controlled by an expert user because even the smallest data misinterpretation might cause misleading results.

In conclusion the proposed procedure, aimed at the assessment and classification of the thermal comfort quality of indoor spaces inside a given building, consists of the following steps:

1. thermal simulation of the building so that indoor environmental parameters may be determined with a selected time step during a whole year;
2. definition of a spatial domain by singling out a set of points suitably distributed over the floor area of the investigated spaces; these points constitutes the vertexes of the mesh that has to be designed to properly put under investigation both irradiated and not irradiated positions inside the studied indoor environment;
3. calculation of MRT over the selected set of points and with the selected time step for a year;
4. thermal comfort assessments using the same temporal and spatial domains defined at steps 1 and 2;
5. calculation of the Environmental Quality Index at every point of the greed designed at step 2;
6. definition of feasible comfort quality classes and environmental classification of the indoor spaces.

In this study the procedure is applied considering both irradiated and non-irradiated subject.

2.1 The mean radiant temperature algorithm

The mean radiant temperature has to be evaluated in two different cases: a) in the case of an un-irradiated subject; b) in the case of a subject irradiated by the solar radiation.

In the case of unirradiated subject the following relation [27] may be utilized:

$$\bar{t}_{r,u} = \sqrt[4]{\sum_{i=1}^{N} F_{S\to i}(t_i + 273)^4} - 273 \tag{1}$$

instead, in the case of subject irradiated by the solar radiation, MRT can be calculated by means of the equation [28]:

$$\bar{t}_{r,i} = \sqrt[4]{\sum_{i=1}^{N} F_{S\to i}(t_i + 273)^4 + \frac{C_{dn}}{\varepsilon\sigma}\left(\alpha_{irr,d}\sum_{j=1}^{M} F_{S\to j} I_{d,j}^{in} + C_S^{in}\alpha_{irr,b} f_p I_{bn}^{in}\right)} - 273 \tag{2}$$

Where the meaning of the variables is reported in the nomenclature section.

The day–night coefficient, C_{dn}, assumes value 1 in diurnal periods and 0 at night time; the indoor building shield coefficient, C_S^{in},assumes value 1 if the subject is hit by the solar radiation beam and 0 otherwise.

The calculation of the angle factors and of the projected area factors may be realized by means of analytical models [29, 30]. On the other hand shading effects caused by the building envelope may lead to a partial reduction of the solar radiation; therefore it is necessary to verify, for each point of the floor, if it is hit by the solar radiation beam: this occurs if the point is situated inside an irradiated zone placed in the environment.

The co-ordinates of the points A, B, C and D (Figure 1) which limit the irradiated zone can be calculated using the expressions reported in Table 1.

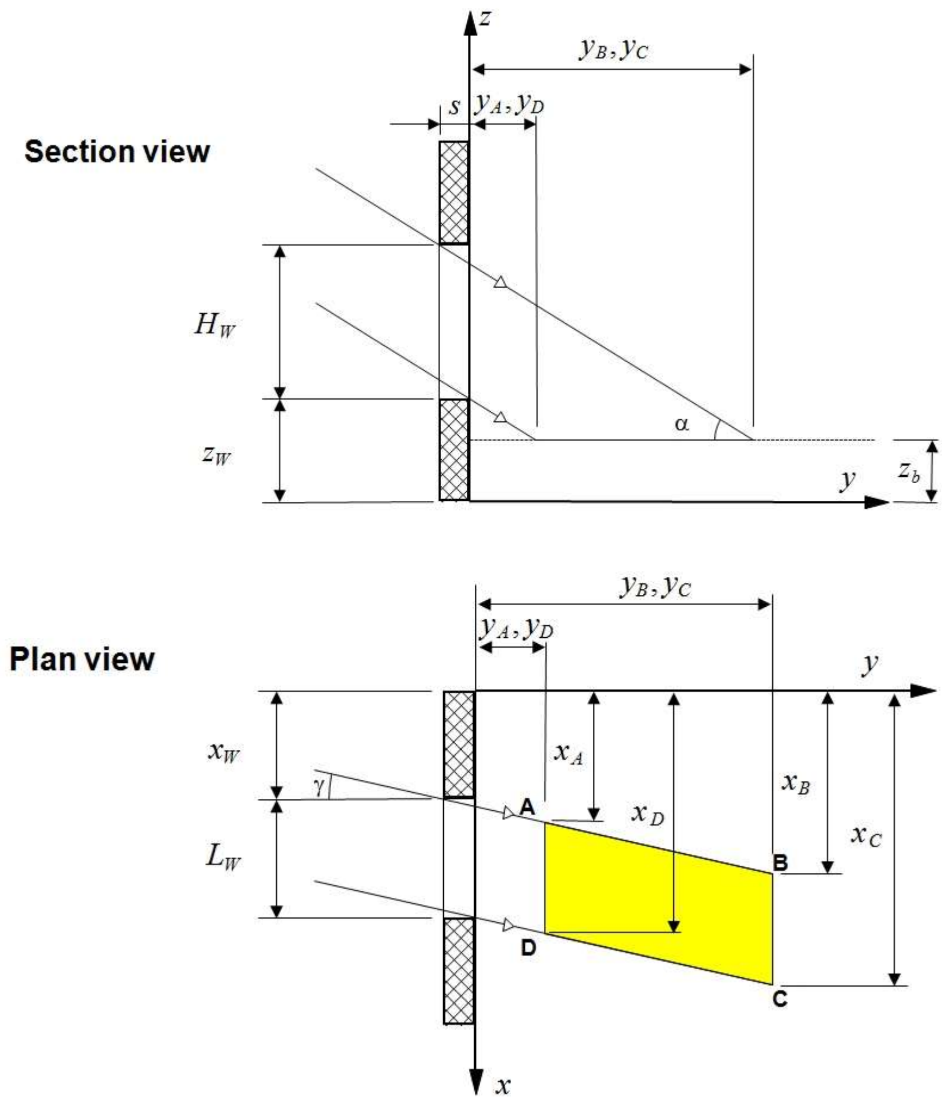

Figure 1. Definition of the geometric parameters involved in the delimitation of the irradiated zone.

Table 1. Coordinates of the points limiting the irradiated zone inside the indoor environment [24].

Point	*x* coordinate	*y* coordinate
A	$x_A = x_W + \left(\frac{z_W - z_b}{\tan\alpha}\cos\gamma + \frac{s}{2}\right)\tan\gamma + \left\lvert\frac{s}{2}\tan\gamma\right\rvert$	$y_A = \frac{z_W - z_b}{\tan\alpha}\cos\gamma$
B	$x_B = x_W + \left(\frac{H_W + z_W - z_b}{\tan\alpha}\cos\gamma - \frac{s}{2}\right)\tan\gamma + \left\lvert\frac{s}{2}\tan\gamma\right\rvert$	$y_B = \frac{H_W + z_W - z_b}{\tan\alpha}\cos\gamma - s$
C	$x_C = x_W + L_W + \left(\frac{H_W + z_W - z_b}{\tan\alpha}\cos\gamma - \frac{s}{2}\right)\tan\gamma - \left\lvert\frac{s}{2}\tan\gamma\right\rvert$	$y_C = \frac{H_W + z_W - z_b}{\tan\alpha}\cos\gamma - s$
D	$x_D = x_W + L_W + \left(\frac{z_W - z_b}{\tan\alpha}\cos\gamma + \frac{s}{2}\right)\tan\gamma - \left\lvert\frac{s}{2}\tan\gamma\right\rvert$	$y_D = \frac{z_W - z_b}{\tan\alpha}\cos\gamma$

In the designed procedure Mean Radiant Temperature must be calculated at different points inside the studied indoor environment in order to take into account the space variability of the radiant field. Therefore, while the height of the calculation points, coinciding with the quote of barycentre of the human body z_b, is fixed by the subject's posture (standing or seated), their position over the horizontal plane (identified by the x and y coordinates) must be individuated to properly consider both irradiated and not irradiated areas. Consequently the floor area of the indoor environment is to be modeled by means of a grid of points designed to suitably cover the space variability of the radiant field. A grid structured as a square mesh with 1 m side length may be appropriate for the most common cases.

Moreover, since solar radiation varies with time for intensity and direction of the beam, the time variability of the radiant field must be considered as well. Hence, at every point of the designed grid the MRT must be assessed with an appropriate time step for a whole year in order to take into account both the daily and seasonal variability of the phenomenon. An hourly time step may be judged appropriate for that purpose.

In regard to the intensity of solar radiation entering the indoor environment through glazed surfaces, it may be calculated considering the optical transmittance of the glass by means of the equations:

$$\mathrm{I_d^{in}} = \tau_\mathrm{d} \times \mathrm{I_d^{out}} \tag{3}$$

$$\mathrm{I_b^{in}} = \mathrm{C_s^{out}} \times \tau_\mathrm{b} \times \mathrm{I_b^{out}} \tag{4}$$

where:

- I_d^{out} and I_b^{out} are the diffuse and the direct component of solar radiation hitting the external side of the glazed surfaces;
- τ_d and τ_b are the optical transmittance of the glass for the diffuse and direct component rispectively and have been calculated using the procedure proposed by ASHRAE [12];
- $\mathrm{C_s^{out}}$ is a shading coefficient taking into account external obstacles to the solar beam component.

2.2 Thermal Comfort Assessment

Comfort condition are assessed by means of Fanger’s methodology [9] based on PMV and PPD indexes.

As far as PMV an PPD indexes are concerned, obviously their values must be evaluated at each point of the grid designed for the MRT assessments and should be related to the same temporal domain. Therefore the analysis should concern a whole year with a calculation time step of one hour.

The PPD and PMV equations are reported in the ISO 7730 Standard [16] and depend on the following parameters [31]:

- M metabolic rate (met);

- I_{cl} clothing insulation (clo);
- t_a air temperature (°C);
- v_a air velocity (m/s);
- p_a water vapour partial pressure (Pa);
- $\bar{t}_r$ mean radiant temperature (°C).

2.3 Calculation of the Environmental Quality Index

The EN 15251 standard [15] introduces methodological hypothesis regarding the evaluation of the environmental quality. In particular the EN 15521 standard introduces a classification of indoor environments based on four levels of quality (I, II, III and IV) which, as far as the thermal facet is concerned, are related to the values of the PPD index (Table 2). This method has been used to assess the Environmental Quality Index (EQI).

Table 2. Environmental quality levels and corresponding PPD boundary values [15].

Quality Level	**Description**	**PPD (%)**
I	High level of expectation and is recommended for spaces occupied by very sensitive and fragile persons with special requirements.	≤6
II	Normal level of expectation and should be used for new buildings and renovations.	6-10
III	Acceptable, moderate level of expectation and may be used for existing buildings.	10-15
IV	Values outside the criteria for the above categories: this category should only be accepted for a limited part of the year.	>15

The long term analysis carried out in this work is based on the assessment of the temporal frequency with which each quality level occurs at every point of the studied grid. The occurrence frequency ($f_L^{P,T}$) of the generic level L, at point P, during the reference period T may be calculated as $f_L^{P,T} = t_L^{P,T}/T$; where $t_L^{P,T}$ is the duration of the environmental conditions belonging to the level L, at point P, during the reference period T.

As a result of these calculations the *Time Fraction Weighted Mean Vector* [F] is obtained [25]:

$$\{\bar{f}\} = \begin{Bmatrix} f_I^{P,T} \\ f_{II}^{P,T} \\ f_{III}^{P,T} \\ f_{IV}^{P,T} \end{Bmatrix} \qquad (5)$$

Consequently, for each point inside the indoor environment, the procedure leads to the assessment of four dimensionless values which allow to estimate the predominant level of indoor comfort quality (I, II, III or IV).

This vector, eventually, can be processed to obtain a single and simple index, namely the Environmental Quality Index, EQI, variable from 0 to 100 and defined by the following relationship [25]:

$$EQI^{P,T} = 100 \times f_I^{P,T} + 70 \times f_{II}^{P,T} + 35 \times f_{III}^{P,T} \qquad (6)$$

2.4 The comfort quality classes

The last step of the methodology consists in the assignment of the indoor quality class to the environments, making use of the index previously determined.

To reach this goal the seven point scale, from A to G, drawn up in Marino et al. [25] was used (Table 3).

Because of its definition, EQI is a spatial function of the considered point P, consequently the comfort classification is spatially variable.

In order to examine the reliability of the projected procedure, its application to a case study is reported in the following section.

Table 3. Environmental Quality classes as a function of the EQI index [25].

Values of the index EQI	Indoor quality class
90 – 100	A
75 – 90	B
60 – 75	C
45 – 60	D
30 – 45	E
15 – 30	F
0 – 15	G

3 A CASE STUDY

The relevant influence of solar radiation on both building energy consumptions and comfort conditions of an irradiated subject will be analyzed in the following sections applying the described methodology to a case study.

For the analysis purpose a building module, with dimensions 8x5x3 m, has been studied (Figure 2).

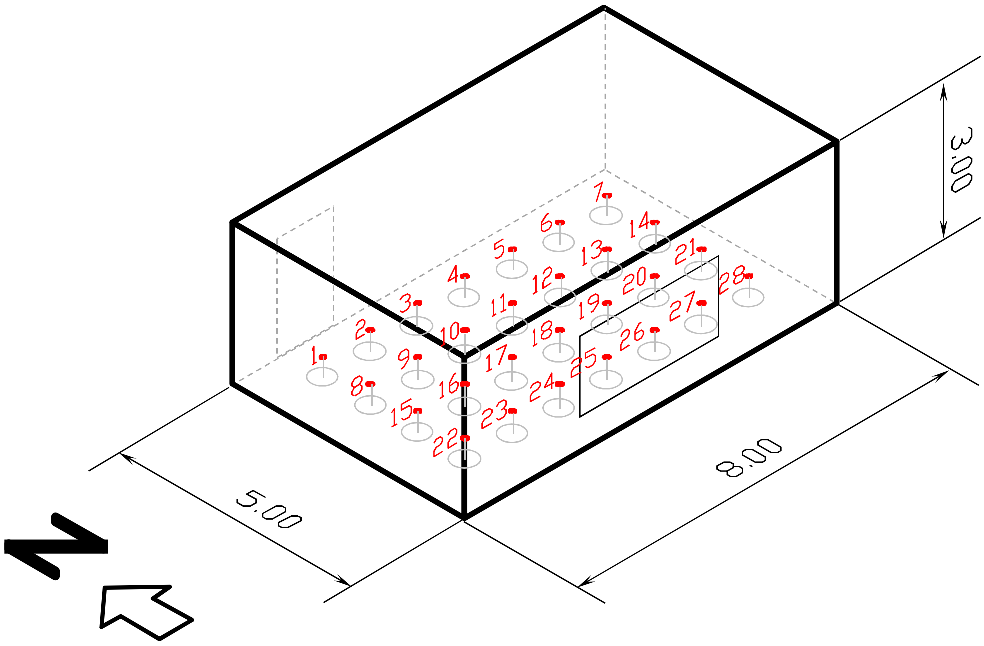

Figure 2. Case Study.

All the structures forming the building envelope are adiabatic except two which are the South and the East exposed walls respectively. They are characterized by a U-factor equal to 0.39 W/m^{2}K and a surface mass of 245 kg/m^2 while the characteristics of each layer composing their structure (i.e. thickness s, thermal conductivity k, density ρ, heat capacity c, and thermal resistance R) are reported in Table 4.

Table 4. Wall layer characteristics.

View	Layer ID	s (m)	k (W/mK)	ρ (kg/m^3)	c (J/kgK)	R (m^{2}K/W)
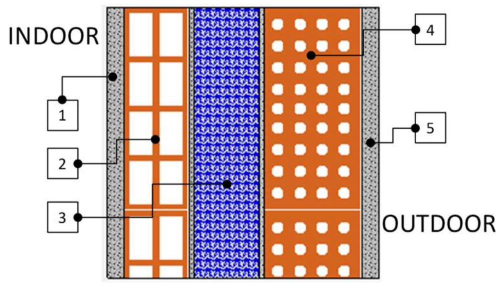	Indoor surface resistance	-	-	-	-	0.130
	1	0.02	0.700	1400	1000	0.029
	2	0.08	-	775	840	0.200
	3	0.08	0.041	30	1200	1.951
	4	0.12	-	1508	840	0.190
	5	0.02	1.400	2000	1000	0.014
	Outdoor surface resistance					0.04

The unique window present, which is South exposed, is 1.5 m high and 3.0 m wide, has an U-factor equal to 2.70 W/m^{2}K and a Solar Heat Gain Coefficient (SHGC) of 0.786. The structure of the glass panel is reported in Table 5 along with the characteristics of each constituting layer (i.e thickness s, thermal conductivity k, thermal resistance R, hemispherical emissivity e, solar reflectance r and solar transmittance t) .

Table 5. Window layer Characteristics.

View	Layer ID	s (m)	k (W/mK)	R (m^{2}K/W)	e	r	t
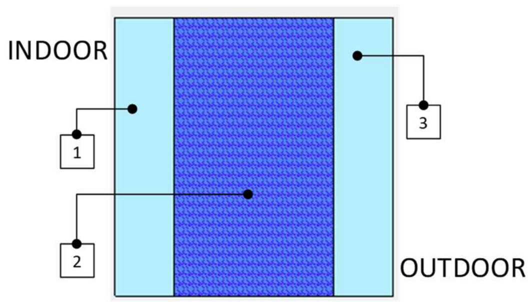	Indoor surface resistance	-	-	0.130	-	-	-
	1	0.006	1.00	0.006	0.84	0.08	0.86
	2	0.016	-	0.188	-	-	-
	3	0.006	1.00	0.006	0.84	0.08	0.86
	Outdoor surface resistance			0.04			

The module, located in Rome, characterized by the climatic conditions reported in Table 6, is equipped with a radiant floor system which can directly extract part of the heat load due to solar radiation coming into the room and transfer it to the water flowing in the pipes [32].

The floor system meets both heating and cooling demands and is controlled by a thermostatic apparatus that keeps the indoor air temperature within a selected range. As regards the control range, two cases were considered: in the first one the control range spans from 20°C to 26°C, in the second one it is defined by the limits of 20°C and 24°C.

As far as the control of the lighting system is concerned, it was assumed that an automatic device turns the lights off when the natural illuminance falls under 300 lux in correspondence of two control points located in middle of the room extent, at a distance of 2 m (point 18) and 4 m (point 4) from the window respectively.

Table 6. Climate conditions of the selected town.

Latitude	Longitude	Yearly dry bulb temperature (°C)		Degree-Days – baseline 18°C	
		Min	Max	Heating	Cooling
41°47′ N	12°13′ E	-4.0	31.8	1525	555

From the point of view of solar control, two configurations of the building module were analyzed: in the first one no shading device was taken into account, while in the second one a completely opaque overhang prevents the space from overheating, especially during summer periods. The overhang has a rectangular structure 3.80 m long and 1.50 m large and is centered with respect to the window symmetry vertical axis.

In summary four cases were analyzed; they are depicted in Table 7 and Figure 3.

Table 7. Analyzed cases

Case	Temperature Control Range (°C)	Shading Device	Sun effect on comfort
0	20-26	NO	No
1	20-26	NO	YES
2	20-26	YES	YES
3	20-24	NO	YES

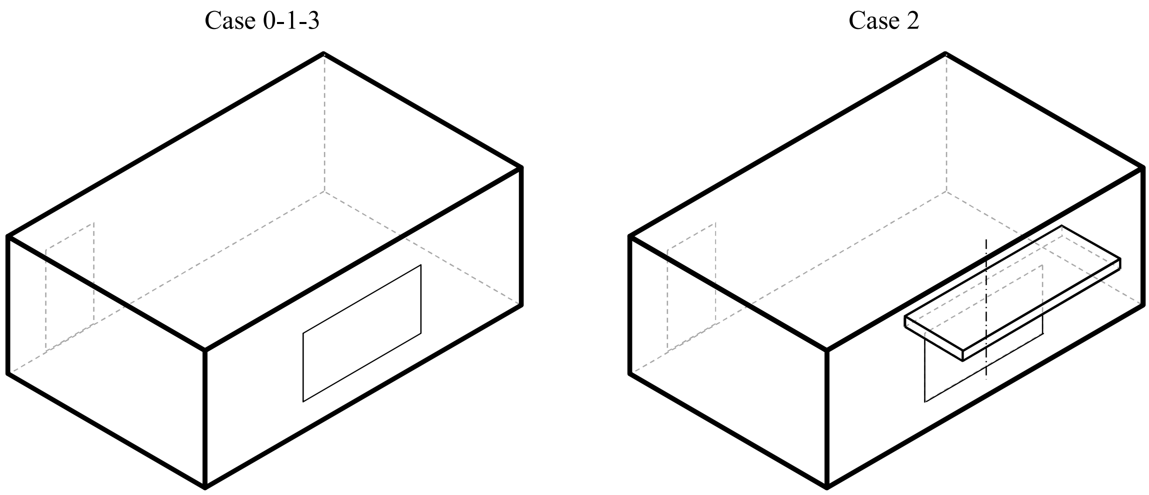

Figure 3. Configurations of the case study with respect to the shading device.

The studied module is of an office building that was considered occupied from 8 a.m. to 5 p.m., from Monday to Friday, while the heating/cooling system was active from 7 a.m. to 5 p.m.. Moreover, in order to assess the comfort conditions of occupants by means of the PPD index, a set of assumptions were made with reference to the needed subjective and physical parameters. In particular it was assumed a metabolic rate value (M) equal to 1.2 met, a relative humidity (RH) of 50%, a constant velocity value of 0.15 m/s and a thermal insulation of the clothing ensemble (I_{cl}) variable from 0.7 clo to 1.0 clo as reported in Table 8.

Table 8. Chosen values of the thermal insulation of the clothing ensemble.

Month	I_{cl} (clo)
January	1.0
February	1.0
March	0.9
April	0.8
May	0.7
June	0.7

July	0.7
August	0.7
September	0.7
October	0.8
November	0.9
December	1.0

A thermal simulation of the building module was carried out by means of the EnergyPlus code, so that the air temperature and the temperature of the wall inner surfaces have been reckoned for a whole year with an hourly time step. Their values have been successively utilized for the evaluation of the MRT and PPD index over a grid of points obtained by patterning the indoor space floor area with a square mesh having a side length of 1 m.

Finally long term evaluations were carried out and hence the comfort level of the indoor environment was classified by means of the EQI defined in the previous section.

3.1 Results

The first stage of the analysis has been aimed at the assessment of the influence of the sun on thermal comfort, therefore Case 0 and Case 1 (Table 7) should be firstly considered.

Figure 4 gives clear evidence of the alterations that might affect the MRT when the solar radiation beaming on the subject is taken into account. In particular, for point 18, located at a distance of 3 m from the North wall and of 4 m from the West wall, the time trend of MRT, assessed with either eq. (1) (unirradiated subject) or eq. (2) (irradiated subject), is plotted.

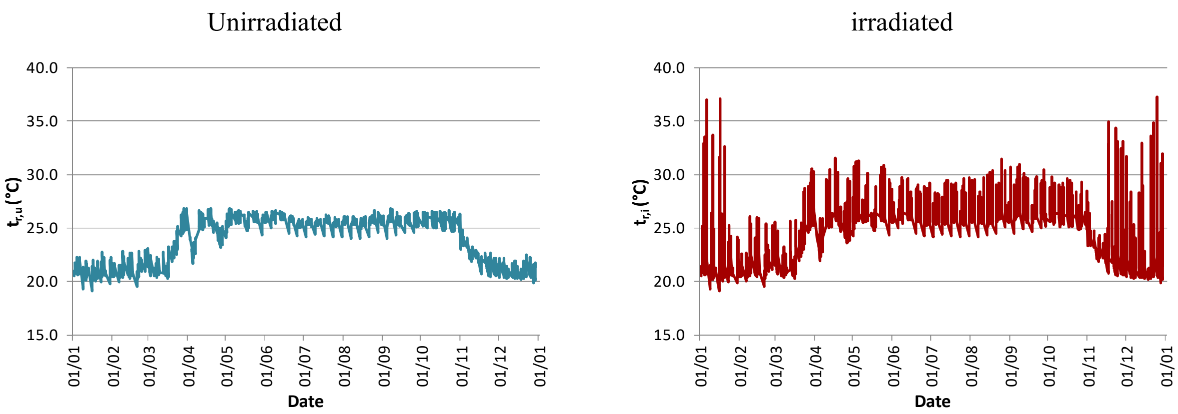

Figure 4. Mean radiant temperature for both unirradiated (Case 0) and irradiated (Case 1) subject (Point 18).

The comparison between the two graphs makes the effect of solar radiation on MRT clear: $t_{r,i}$ is always appreciably higher than $t_{r,u}$, but it must be pointed out that in the winter time, when the sun altitude causes the subject to be hit by the direct component of solar radiation crossing the South exposed window, $t_{r,i}$ remarkably exceeds $t_{r,u}$ and a difference of more than 15°C can been found. Moreover, the effect of this phenomenon on comfort sensation is deducible from Figure 5, where the PPD time trend for both unirradiated and irradiated subject, located at Point 18, is reported. With the exclusion of a short period in April, during the whole year the PPD keeps lower than 20% in the case of an unirradiated subject but it remarkably rises up if the solar radiation is taken into account.

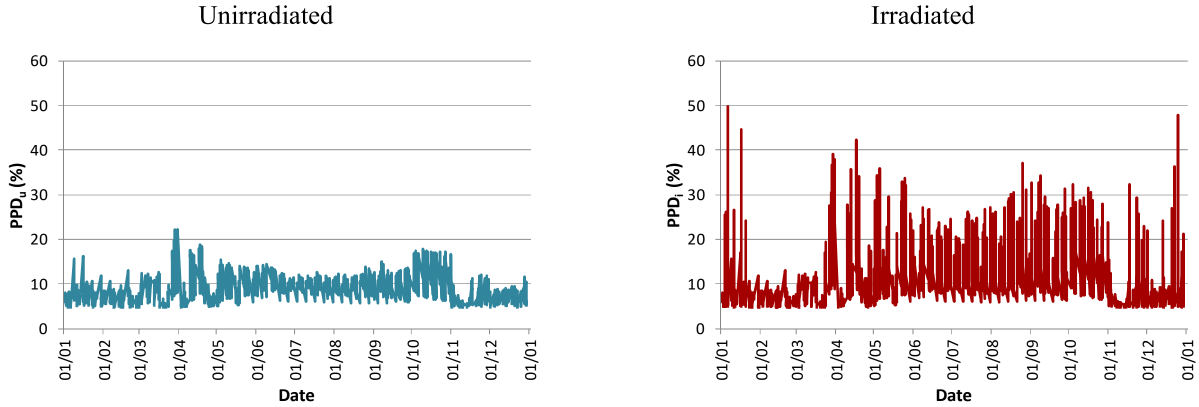

Figure 5. PPD index for both unirradiated (Case 0) and irradiated (Case 1) subject (Point 18).

Indeed this phenomenon affects the comfort classification to a relevant extent; this is shown in Figure 6, which reports the frequencies $f_I^{P,month}$, $f_{II}^{P,mon}$, $f_{III}^{P,month}$, $f_{IV}^{P,month}$ as they evolve at Point 18 when the effect of the sun is considered, and in Figure 7 which highlights, with a monthly base, the influence of solar radiation on the values of the EQI at the same Point 18.

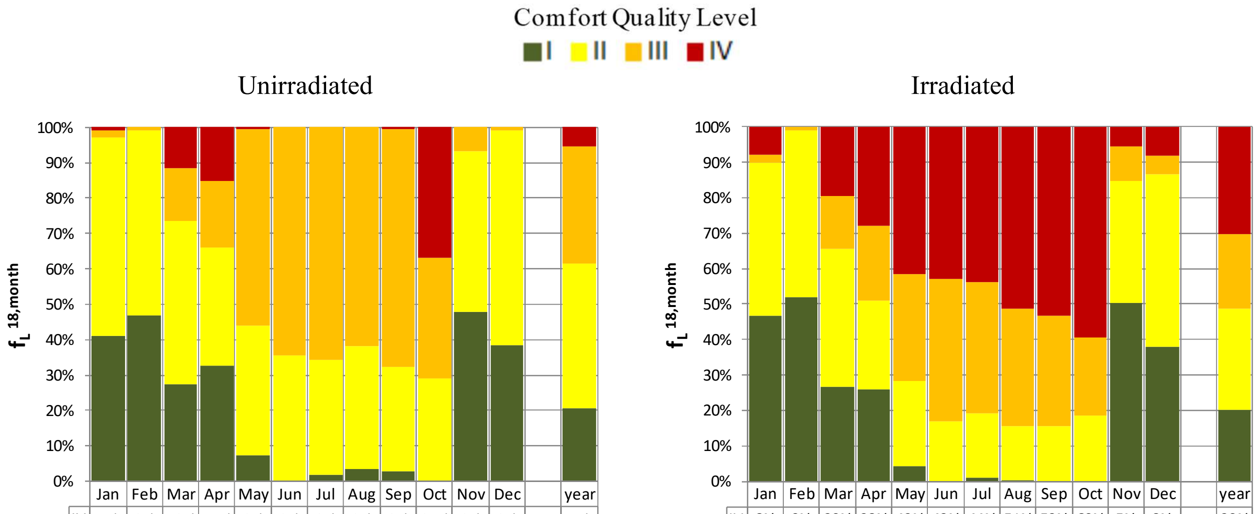

Unirradiated

	Jan	Feb	Mar	Apr	May	Jun	Jul	Aug	Sep	Oct	Nov	Dec		year
IV	1%	0%	12%	15%	0%	0%	0%	0%	0%	37%	0%	0%		5%
III	2%	1%	15%	19%	56%	65%	66%	62%	67%	34%	7%	1%		33%
II	56%	52%	46%	34%	37%	35%	32%	35%	30%	29%	45%	60%		41%
I	41%	47%	27%	33%	7%	0%	2%	3%	3%	0%	48%	39%		21%

Irradiated

	Jan	Feb	Mar	Apr	May	Jun	Jul	Aug	Sep	Oct	Nov	Dec		year
IV	8%	0%	20%	28%	42%	43%	44%	51%	53%	60%	5%	8%		30%
III	2%	1%	15%	21%	30%	40%	37%	33%	31%	22%	10%	5%		21%
II	43%	47%	39%	25%	24%	17%	18%	15%	16%	19%	34%	49%		29%
I	47%	52%	27%	26%	4%	0%	1%	0%	0%	0%	50%	38%		20%

Figure 6.Occurrence frequencies $f_I^{18,month}$, $f_{II}^{18,month}$, $f_{III}^{18,mon}$, $f_{IV}^{18,month}$ at Point 18, for both unirradiated (Case 0) and irradiated (Case 1) subject.

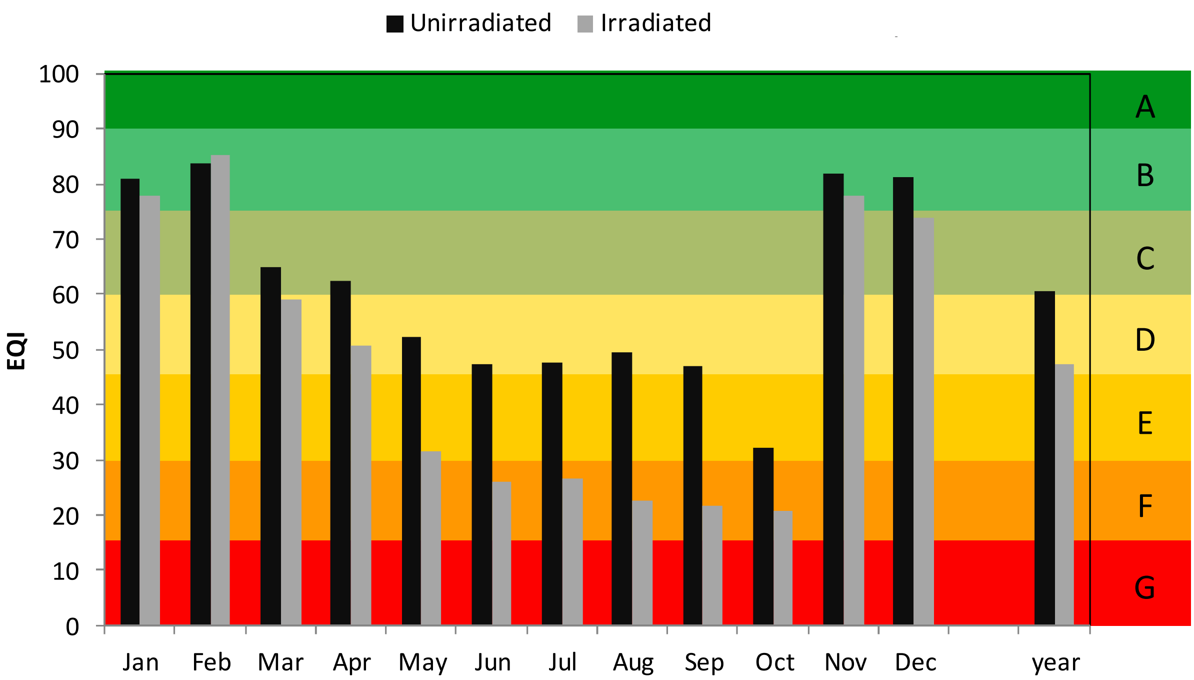

Figure 7. EQI at Point 18 during the different months and whole year, for both unirradiated (Case 0) and irradiated (Case 1)subject.

It is worth pointing out that the effect of the sun, while might occasionally improve the comfort level in winter (cf. February in Figure 7), generally acts lowering the comfort quality class in summer, spring, autumn and, hence, during the whole year.
Similar occurrences can be observed in correspondence of the various 28 points that pattern the floor area of the building module so that if the analysis is extended to the whole room, the maps reported in Figures 8-10 may be obtained.
The curves represented in the figures are the iso-EQI curves, namely the locus of points where EQI, during the selected period (month or year), assumes the same value.

The reported maps highlight that, due to the position of the window, the effect of the sun is remarkably noticeable in the central area (Figure 8) of the room and, while during winter it concerns mainly the farthest points from the window (Figure 9), during summer it involves the region next to the South wall (Figure 10) because of the different inclination of the sun rays during the various seasons.

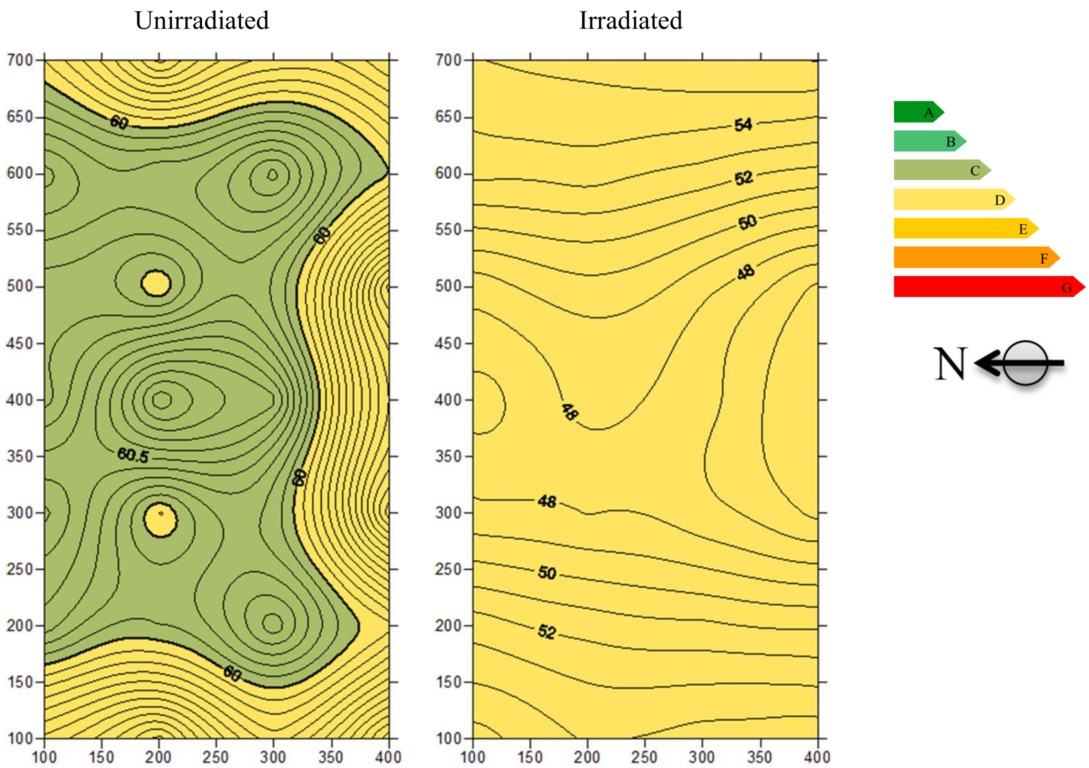

Figure 8. Iso-EQI curves for both unirradiated (Case 0) and irradiated (Case 1)subject. Reference period: year

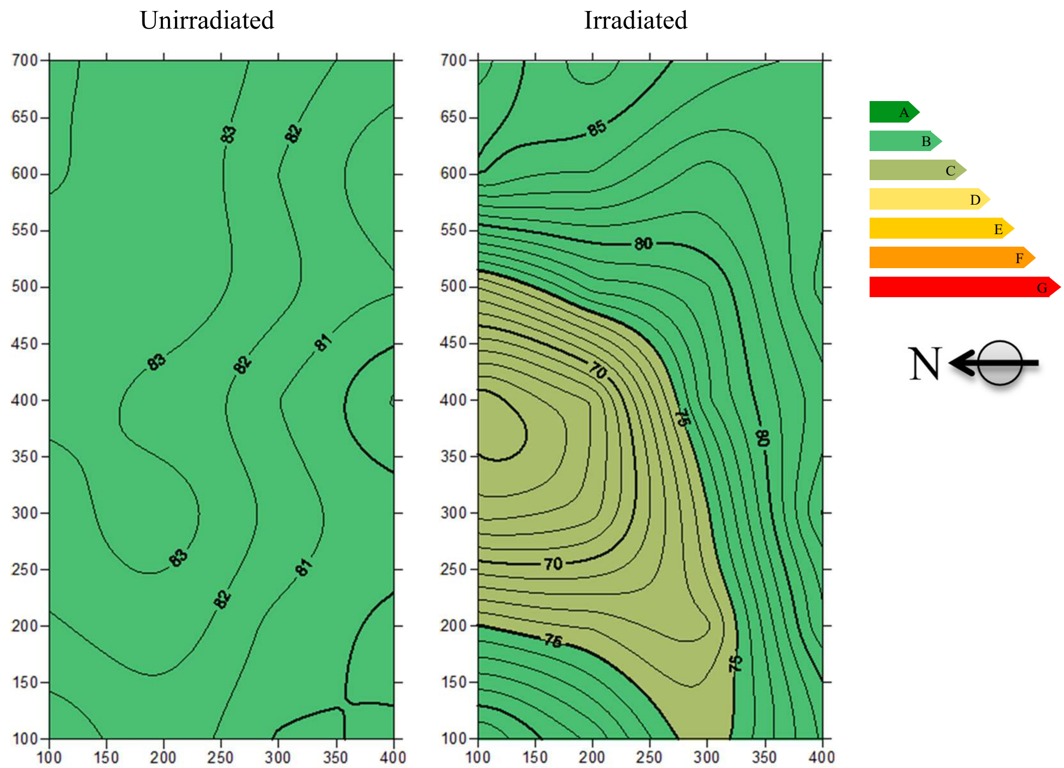

Figure 9. ISO-EQI curves for both unirradiated (Case 0) and irradiated (Case 1)subject. Reference period: January

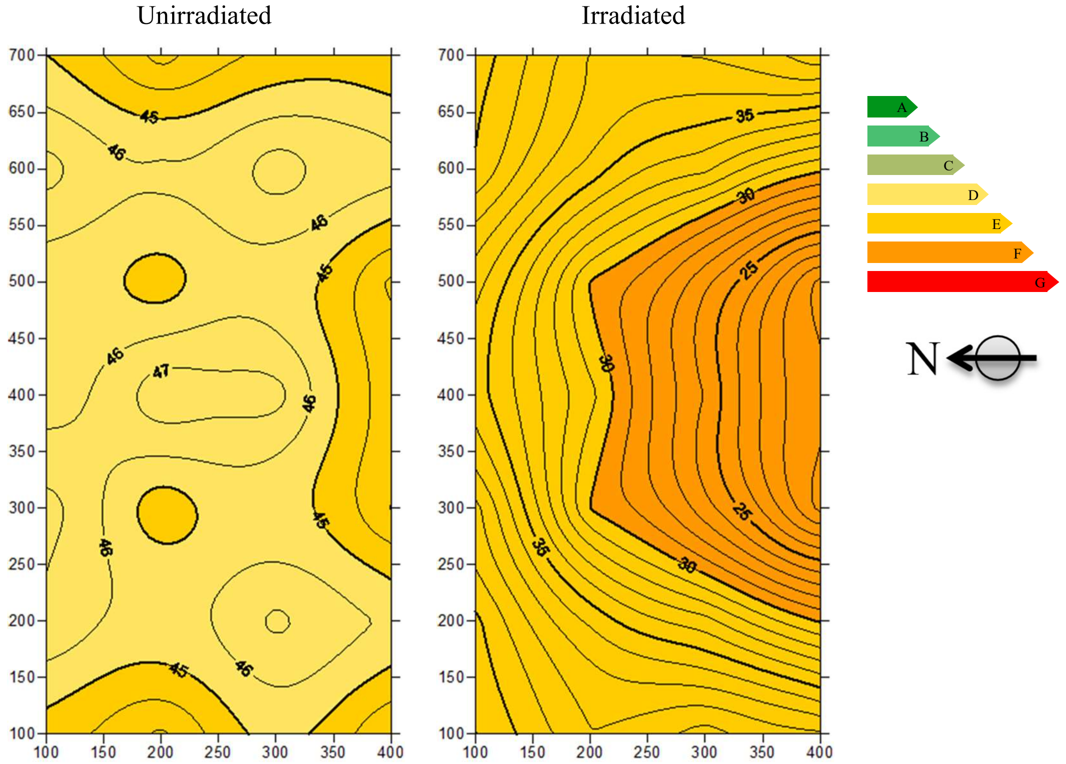

Figure 10. ISO-EQI curves for both unirradiated (Case 0) and irradiated (Case 1)subject. Reference period: June

In summary the influence of the sun on comfort classification might also be derived from Figure 11 and Figure 12 which report the percentage of floor area in which every class occurs.

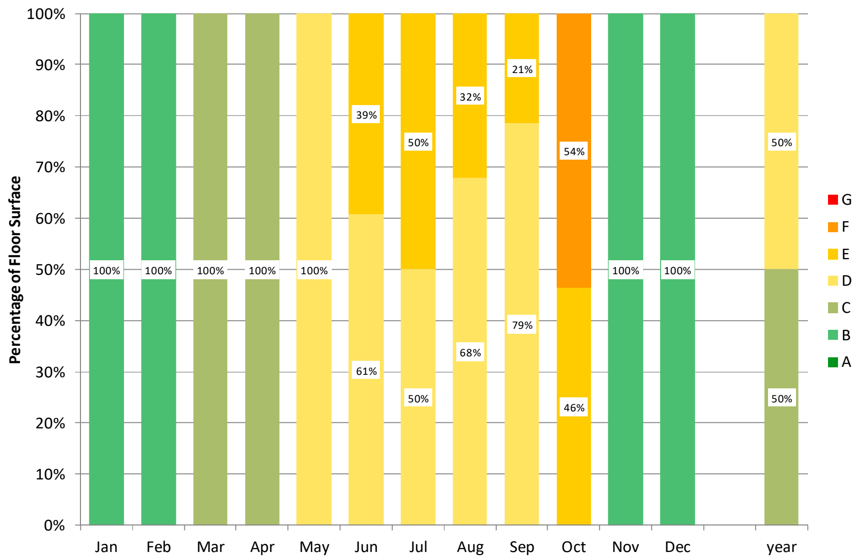

Figure 11. Environmental classification: comfort class distribution over the floor surface for unirradiated (Case 0) subject.

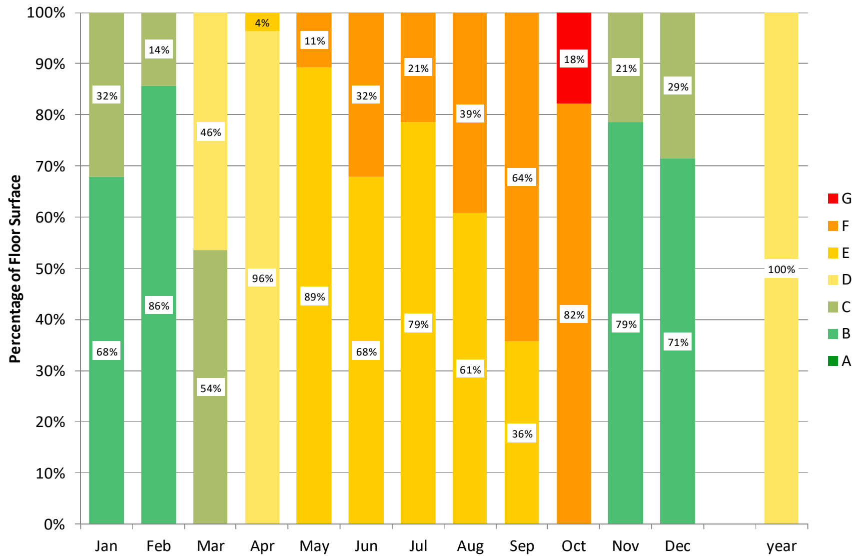

Figure 12. Environmental classification: comfort class distribution over the floor surface for irradiated (Case 1) subject.

In the long term (year), when the sun effects are not considered, the environmental conditions inside the studied room are classifiable as C in correspondence of the 50% of the floor area and D over the remaining 50% (Figure 11), but they worsen entirely towards class D when the sun is taken into account (Figure 12).

In order to analyze some of the available solutions usually planned to either limit or compensate the negative impact of the sun, two cases were considered and compared: firstly the effect of the overhang (Figure 3) described in the previous section was assessed (Case 2 - Table 7), successively the consequence of lowering the cooling set-point temperature to 24°C (Case 3 - Table 7) was investigated.

The results are reported in Figure 13 and Figure 14.

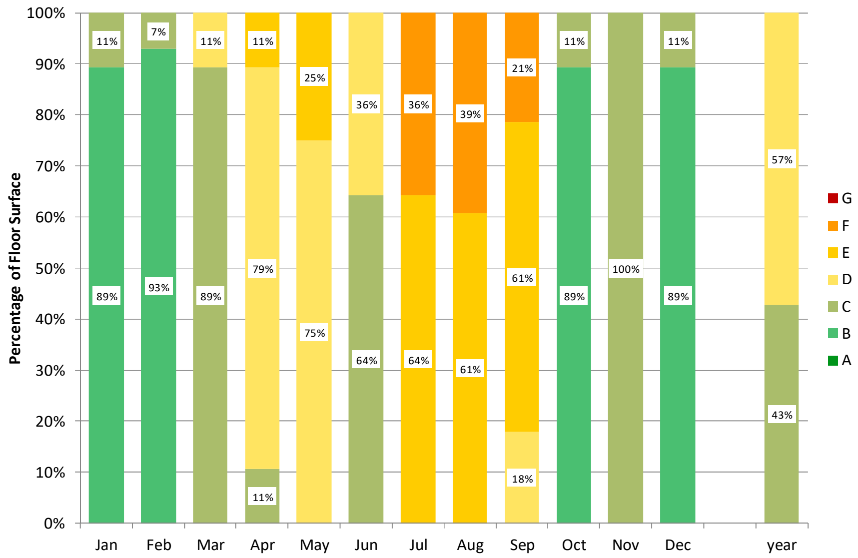

Figure 13. Environmental classification: comfort class distribution over the floor surface. The overhang is on (Case 2).

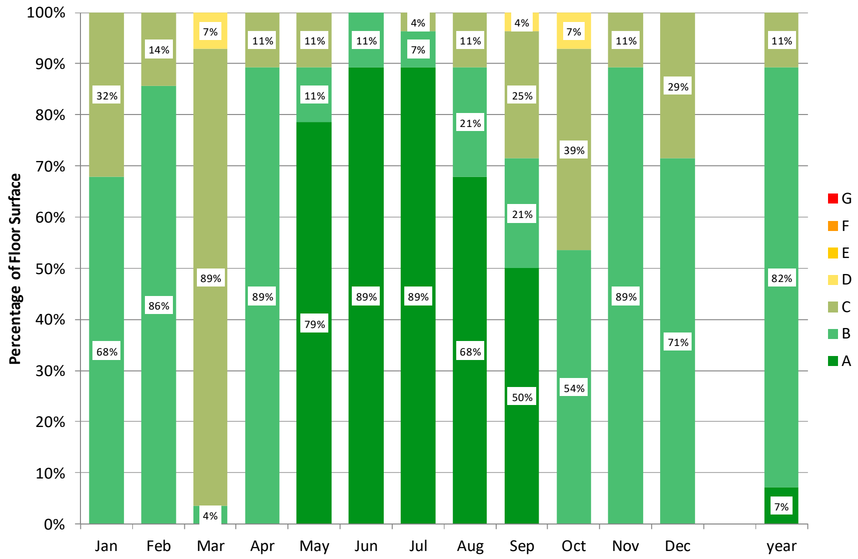

Figure 14. Environmental classification: comfort class distribution over the floor surface. The cooling temperature set-point is set to 24°C (Case 3).

Objectively, on an annual basis, the overhang acts improving the environmental condition (Case 2 - Figure 13), almost restoring the classes that were found when no sun effect was taken into account (Case 0 - Figure 9).

On the other hand, the reduction of the cooling air temperature set-point (Case 3 - Figure 14) improves the comfort quality level of the environment to a large extent.

As far as energy consumption is concerned, Figures 15-17 show the results for the analyzed cases in terms of monthly primary energy.

According to the results of several simulation studies [33] overheating due to high solar irradiation could cause higher energy use in summer, making the use of external or/and internal shading essential for energy saving purposes.

As expected, a reduction of the energy consumptions for cooling (Q_C) has been found with the installation of the overhang (Case 2), while, on the contrary, the reduction of the temperature set-point (Case 3) has made the cooling energy demand higher. As regards the heating energy consumption (Q_H), it is enhanced by the presence of the overhang (Case 2), but, of course, it is not influenced by the change of the cooling set-point (Case 3).

From the point of view of the lighting demand (Q_L), the presence of the overhang causes an appreciable increase of the energy consumptions. Nevertheless both spring and summer months are not affected by this phenomenon because the long duration of the daylight makes the activation of the lighting system however less likely.

A summary of the results in terms of both comfort conditions and primary energy consumptions is shown in Figure 18 where, for each analyzed case, the yearly energy demand and the values of EQI_{avg} are reported.

EQI_{avg} is an average EQI obtained as follows

$$EQI_{avg}^{T} = \frac{\sum_{P} EQI^{P,T}}{n_P} \tag{7}$$

where P is the generic point T the reference period and n_p the number of considered points.

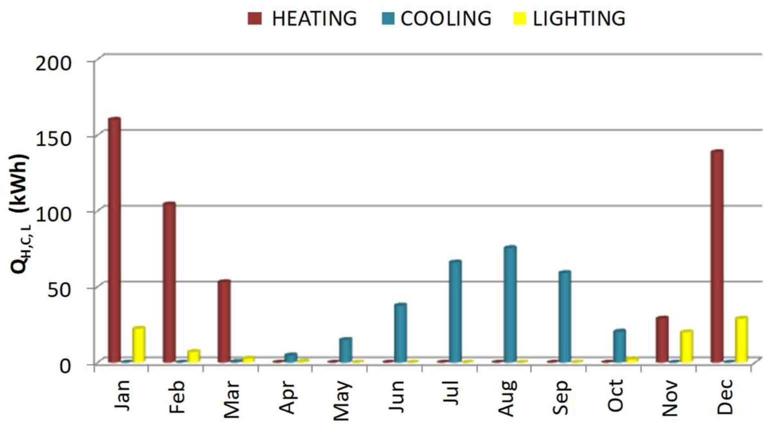

Figure 15. Cooling heating and lighting primary energy consumptions. Case 0 and Case 1.

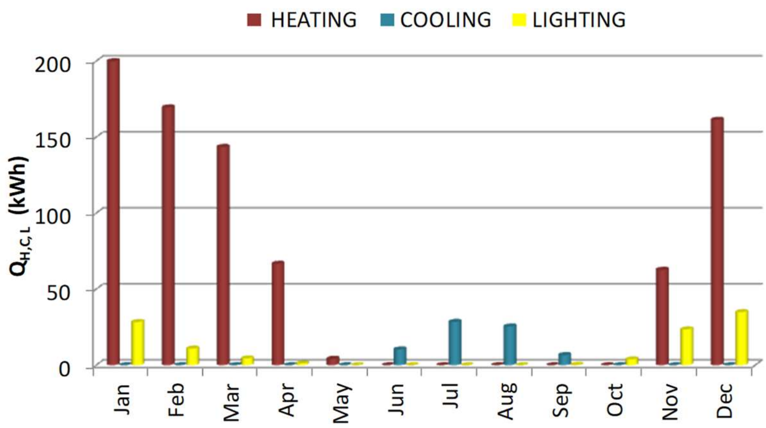

Figure 16. Cooling heating and lighting primary energy consumptions. Case 2.

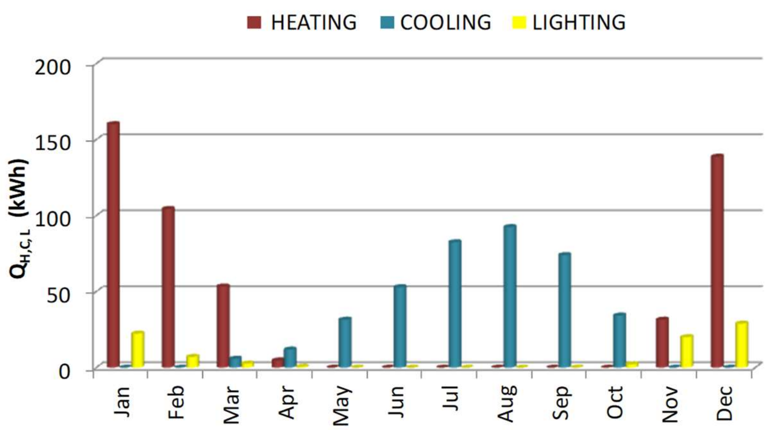

Figure 17. Cooling heating and lighting primary energy consumptions. Case 3.

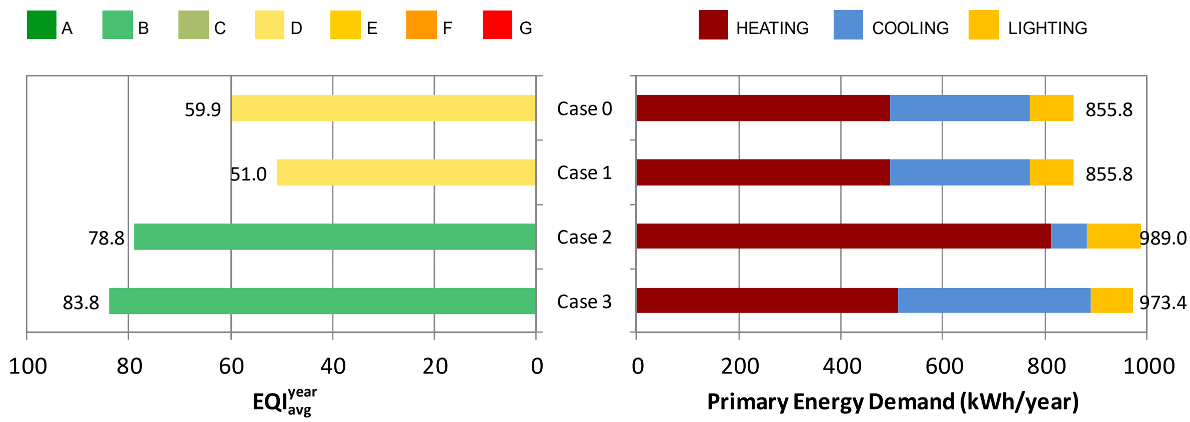

Figure 18. Environmental classification and primary energy demand.

4 CONCLUSION

The current work designs a procedure which allows the rating of the thermal comfort quality of indoor environments in presence of solar radiation. It could be used in correlation with energy classification of buildings in order to refer energy performance to indoor environmental conditions, as stated by 2010/31/EU European Directive [5].

The most innovative facet of the proposed procedure lies in the consideration of solar radiation hitting the subject that affects thermal comfort to a large extent. Indeed, given that solar radiation entering into indoor environment and shining on the occupants, strongly depends on the position of the subjects, period of the year and time of the day, the proposed methodology provides for a spatial and long term analysis that covers one year at least.

The application to a case study has demonstrated that solar radiation may cause the presence of unacceptable environmental conditions in a remarkably large portion of the studied indoor space. The phenomenon would have not been noticed if solar radiation had not been taken into account using the proposed algorithm. Obviously, the issue might be stemmed by the use of solar shields, but this solution must be carefully analyzed because, in spite of the improvement of the comfort conditions, it may cause the enhancement of the energy demand of buildings. Therefore their operational mode must be accurately designed as a result of the trade-off between energy saving and comfort needs and in consideration of the weather conditions, building-plant configuration, management and intended use conditions of the indoor environments, etc..

For the case analyzed in the present study, for example, the designed solar shield, which was an overhang installed over the South exposed window, has proved to be less effective than changing the cooling temperature and this result concerns both point of views of energy consumptions and environmental comfort.

These conclusions should be taken into account when optimization processes are designed. As a matter of fact, in order to avoid misleading results, the analysis aimed at the identification of the optimal building-system configuration should regard both comfort and energy facet and, above all, it should be able to properly assess the time and space variations of the involved variables. This last circumstance allows an appropriate evaluation of the effect of the weather conditions and especially of solar radiation which proved to affect results to a remarkable extent.

By means of such an analysis, the presence of non-comfortable positions inside the studied indoor environment can be highlighted and the frequency of their occurrence can be assessed, so that the arrangement of the tasks and of the organization of the human activities to be performed inside the room become part of the optimization process.

As a consequence, whereas the definition of the optimal configuration become strictly connected to the singular studied situation and cannot be generalized, the reliability of the result improves.

The proposed methodology is suitable for this type of analysis and, hence, for optimization purposes because it allows proper analysis of both time and space performances of every examined configuration, so that the effect of weather conditions and especially of sun irradiation are able to be taken into account appropriately.

As regards the presence of unacceptable environmental conditions due to solar radiation entering through glazed surfaces, movable and automated shields or switchable glass, controlled by smart systems able to both follow the values of some environmental variable (MRT, solar radiation ,etc.) and react accordingly, could be effective solutions and, of course, they should be taken into account as part of the optimization process; therefore future analysis will be planned in this direction.

REFERENCES

[1] T. Akimoto, S. Tanabe, T. Yanai, M. Sasaki, Thermal comfort and productivity - Evaluation of workplace environment in a task conditioned office, Building and Environment, 45 (2010) 45-50.
[2] C.-A. Roulet, Indoor environment quality in buildings and its impact on outdoor environment, Energy and Buildings, 33 (2001) 183-191.
[3] J.F. Nicol, M.A. Humphreys, Adaptive thermal comfort and sustainable thermal standards for buildings, Energy and Buildings, 34 (2002) 563-572.
[4] European Union, Directive 2002/91/EC of the European Parliament and of the Council of 16 december 2002 on the energy performance of buildings, in, Official Journal of the European Communities, Strasbourg, 2006.
[5] European Union, Directive 2010/31/EU of the European Parliament and of the Council of 19 May 2010 on the energy performance of buildings, in, Official Journal of the European Communities, Strasbourg, 2010.
[6] F.R. d'Ambrosio Alfano, B.I. Palella, G. Riccio, The role of measurement accuracy on the thermal environment assessment by means of PMV index, Building and Environment, 46 (2011) 1361-1369.
[7] Seppänen O., Fisk W.J., F. D., Cost benefit analysis of the night-time ventilative cooling, in: Proceedings of the Healthy Buildings 2003 Conference, Singapore, 2003, pp. 394-399.
[8] Seppänen O., Fisk W.J., Faulkner D., L. Q.H., Room temperature and productivity in office work, in: Proceedings of the Healthy Buildings 2006 Conference, Lisbon, 2006, pp. 243-247.
[9] P.O. Fanger, Thermal Comfort, McGraw-HiIl, Danish Technical Press, Copenhagen, 1970.
[10] A.P. Gagge, A.P. Fobelets, L.G. Berglund, A standard predictive index and human response to the thermal environment, in, ASHRAE Transactions, 1986, pp. 709-731.
[11] M. Hamdi, G. Lachiver, F. Michaud, A new predictive thermal sensation index of human response, Energy and Buildings, 29 (1999) 167-178.
[12] ASHRAE, ASHRAE handbook-fundamentals, American Society of Heating, Refrigerating and Air-Conditioning Engineers, 2001.
[13] R. de Dear, S.G. Brager, The adaptive model of thermal comfort and energy conservation in the built environment, International Journal of Biometeorology, 45 (2001) 100-108.
[14] R. Yao, B. Li, J. Liu, A theoretical adaptive model of thermal comfort â€“ Adaptive Predicted Mean Vote (aPMV), Building and Environment, 44 (2009) 2089-2096.
[15] CEN, EN 15251 - Indoor environmental input parameters for design and assessment of energy performance of buildings - addressing indoor air quality, thermal environment, lighting and acoustics, in, European Standardisation Organisation, Bruxelles, 2007.
[16] ISO, EN ISO 7730 - Ergonomics of the thermal environment - Analytical determination and interpretation of thermal comfort using calculation of the PMV and PPD indices and local thermal comfort criteria, in, International Standard Organization, Geneva, 2005.
[17] M.C. Singh, S.N. Garg, R. Jha, Different glazing systems and their impact on human thermal comfortâ€"Indian scenario, Building and Environment, 43 (2008) 1596-1602.
[18] I. Atmaca, O. Kaynakli, A. Yigit, Effects of radiant temperature on thermal comfort, Building and Environment, 42 (2007) 3210-3220.

[19] M. Bessoudo, A. Tzempelikos, A.K. Athienitis, R. Zmeureanu, Indoor thermal environmental conditions near glazed facades with shading devices â€“ Part I: Experiments and building thermal model, Building and Environment, 45 (2010) 2506-2516.
[20] A. Tzempelikos, M. Bessoudo, A.K. Athienitis, R. Zmeureanu, Indoor thermal environmental conditions near glazed facades with shading devices â€“ Part II: Thermal comfort simulation and impact of glazing and shading properties, Building and Environment, 45 (2010) 2517-2525.
[21] D.H. Kang, P.H. Mo, D.H. Choi, S.Y. Song, M.S. Yeo, K.W. Kim, Effect of MRT variation on the energy consumption in a PMV-controlled office, Building and Environment, 45 (2010) 1914-1922.
[22] S.G. Hodder, K. Parsons, The effects of solar radiation on thermal comfort, International Journal of Biometeorology, 51 (2007) 233-250.
[23] E. Arens, L. Huang, T. Hoyt, X. Zhou, H. Zhang, S. Schiavon, Modeling the comfort effects of short-wave solar radiation indoors, in: Proceedings of Indoor Air 2014, Hong Kong, July 7-12, 2014.
[24] M. La Gennusa, A. Nucara, M. Pietrafesa, G. Rizzo, A model for managing and evaluating solar radiation for indoor thermal comfort, Solar Energy, 81 (2007) 594-606.
[25] C. Marino, A. Nucara, M. Pietrafesa, Proposal of comfort classification indexes suitable for both single environments and whole buildings, Building and Environment, 57 (2012) 58-67.
[26] D.B. Crawley, L.K. Lawrie, C.O. Pedersen, R.K. Strand, R.J. Liesen, F.C. Winkelmann, W.F. Buhl, Y.J. Huang, A.E. Erdem, D.E. Fisher, M.J. Witte, J. Glazer, EnergyPlus: Creating a New-Generation Building Energy Simulation Program, Energy and Buildings, 33 (2001) 339-331.
[27] ISO, EN ISO 7726 - Ergonomics of the thermal environment - Instruments for measuring physical quantities, in, International Standard Organization, Geneva, 1998.
[28] M. La Gennusa, A. Nucara, G. Rizzo, G. Scaccianoce, The calculation of the mean radiant temperature of a subject exposed to the solar radiation—a generalised algorithm, Building and Environment, 40 (2005) 365-373.
[29] G. Rizzo, G. Cannistraro, G. Franzitta, Algorithms for the calculation of the view factors between persons and rectangular surfaces in parallelepiped environments, Energy and Buildings, 19 (1992) 51-60.
[30] G. Franzitta, G. Rizzo, G. Cannistraro, Algorithms for the calculation of the mean projected area factors of seated and standing persons, Energy and Buildings, 17 (1991) 221-230.
[31] ISO, EN ISO 13731 - Ergonomics of the thermal environment - Vocabulary and symbols, in, International Standard Organization, Geneva, 2001.
[32] M. De Carli, M. Tonon, Effect of modelling solar radiation on the cooling performance of radiant floors, Solar Energy, 85 (2011) 689-712.
[33] D.A. Chwieduk, Some aspects of modelling the energy balance of a room in regard to the impact of solar energy, Solar Energy, 82 (2008) 870-884.

NOMENCLATURE

α	solar altitude angle (°)
$\alpha_{irr,d}$	relative absorbances referring to the diffuse solar radiation (adim)
$\alpha_{irr,b}$	relative absorbances referring to the direct solar radiation (adim)
c	heat capacity (J kg^{-1} K^{-1})
C_{dn}	day–night coefficient (adim)
C_S^{out}	shading coefficient taking into account external obstacles to the solar beam component (adim)
C_S^{in}	indoor building shield coefficient (adim)
e	hemispherical emissivity (adim)
ε	emissivity of the human body (adim)
$EQI^{P,T}$	Environmental Quality Index at point P, during the reference period T (adim)
EQI_{avg}^{T}	environment average of the Environmental Quality Index during the reference period *T* (adim)
f_p	projected area factor of the subject in the solar beam direction (adim)
$F_{S\rightarrow i}$	angle factors between the subject and the i^{th} internal surface (adim)
$F_{S\rightarrow j}$	angle factors between the subject and the j^{th} transparent surface of the envelope (adim)
γ	solar azimuth angle (°)
I_{bn}^{in}	direct component of solar radiation entering the environment through its transparent surfaces and shining on the subject (Wm^{-2})
I_b^{out}	direct component of solar radiation hitting the external side of the glazed surfaces (Wm^{-2})
I_{cl}	clothing insulation (clo)

$I_{d,j}^{in}$	diffuse component of solar radiation entering the environment through its transparent surfaces and shining on the subject (Wm^{-2})
I_d^{out}	diffuse component of solar radiation hitting the external side of the glazed surfaces (Wm^{-2})
k	thermal conductivity ($Wm^{-1}K^{-1}$)
L_W	length of window (m)
M	metabolic rate (met)
$f_L^{P,T}$	occurrence frequency of the category of quality L, at point P, during the reference period T (adim)
H_W	height of window (m)
x_W	abscissa of the lower right corner of a window as viewed by an observer watching it from the inside (m)
p_a	water vapour partial pressure (Pa)
R	thermal resistance ($Wm^{-2}K^{-2}$)
RH	relative humidity (%)
s	wall thickness (m)
r	solar reflectance (adim)
ρ	density (kg m^{-3})
σ	Stefan–Boltzmann constant (5.67×10^{-8} $Wm^{-2}K^{-4}$)
t	solar transmittance (adim)
t_a	air temperature (°C)
t_i	temperature of the i^{th} isothermal surface of the environment (°C)
τ_d	optical transmittance of the glass for the diffuse solar component (adim)
τ_b	optical transmittance of the glass for the direct solar component (adim)
$\bar{t}_{r,u}$	mean radiant temperature of an un-irradiated subject (°C)
$\bar{t}_{r,i}$	mean radiant temperature of a subject irradiated by the solar radiation (°C)
v_a	air velocity (ms^{-1})
x_A, y_A x_B, y_B x_C, y_C x_D, y_D	coordinates of the points limiting the irradiated zone inside the indoor environment (m)
z_b	quote of barycentre of the human body (m)
z_W	quote of the lower right corner of a window as viewed by an observer watching it from the inside (m)